• Intelligent Ophthalmology •

AI-assisted automated interpretation of corneal topography in orthokeratology patients: enhancing diagnostic precision and efficiency

Dao-Huan Kang[1], Lu Yuan[1], Jia Feng[1], Jiao Zhan[1], Andrzej Grzybowski[2], Wen Sun[1], Kai Jin[3]

[1]Department of Ophthalmology, Children's Hospital, Zhejiang University School of Medicine, National Clinical Research Center for Child Health, Hangzhou 310051, Zhejiang Province, China
[2]Institute for Research in Ophthalmology, Foundation for Ophthalmology Development, Poznan 60-001, Poland
[3]Eye Center, the Second Affiliated Hospital, School of Medicine, Zhejiang University, Hangzhou 310006, Zhejiang Province, China
Correspondence to: Wen Sun. Department of Ophthalmology, Children's Hospital, Zhejiang University School of Medicine, National Clinical Research Center for Child Health, Hangzhou 310051, Zhejiang Province, China. drsunwen@zju.edu.cn; Kai Jin. Eye Center, the Second Affiliated Hospital, School of Medicine, Zhejiang University, Hangzhou 310006, Zhejiang Province, China. jinkai@zju.edu.cn
Received: 2025-01-13 Accepted: 2025-09-02

Abstract

● **AIM:** To evaluate the potential of artificial intelligence (AI) for automating corneal topography interpretation in orthokeratology patients, aiming to enhance diagnostic precision, efficiency, and clinical decision-making in myopia management.

● **METHODS:** The 1469 corneal topography images from 582 eyes of 326 myopic children treated with orthokeratology lenses over 47mo were collected. Each sample was categorized by decentration, treatment zone size, shape variation, and eye laterality. A multi-task AI model was developed to predict these parameters, with performance measured using area under curve (AUC), accuracy, and F1 scores. We compared AI-only, human-only, and combined Human+AI approaches on a subset of 100 images. External validation with images from additional hospitals tested model generalizability.

● **RESULTS:** The model achieved high accuracy in eye-side prediction (AUC 0.95) and AUC values of 0.52-0.74 for decentration, treatment zone, and shape variation tasks. The combined Human+AI method outperformed AI-only and human-only approaches, achieving the highest accuracy (up to 87%) and fastest processing time (80ms). External validation confirmed robust performance in simple tasks, though accuracy was lower for complex classifications due to imaging variations.

● **CONCLUSION:** AI provides efficient routine corneal topography assessments, while complex cases benefit most from a Human+AI approach, particularly in scenarios requiring nuanced clinical interpretation. The model currently functions as an assistive tool.

● **KEYWORDS:** artificial intelligence; corneal topography; orthokeratology; myopia management

DOI:10.18240/ijo.2025.12.01

Citation: Kang DH, Yuan L, Feng J, Zhan J, Grzybowski A, Sun W, Jin K. AI-assisted automated interpretation of corneal topography in orthokeratology patients: enhancing diagnostic precision and efficiency. *Int J Ophthalmol* 2025;18(12):2217-2224

INTRODUCTION

Myopia, is increasingly becoming a global health issue, particularly affecting younger people[1-2]. In China, it's estimated that by the middle of the century, around 84% of children and teenagers may develop myopia[3]. This growing trend raises significant concerns for public health, as myopia is linked to serious eye conditions like retinal detachment, glaucoma, and cataracts, which could lead to long-term complications for both individuals and the healthcare system[4-5]. Orthokeratology lens therapy has gained popularity as a non-surgical method for correcting myopia, especially in children[6]. These specially designed lenses are worn overnight to reshape the cornea, allowing for clear vision during the day without the need for glasses or daytime contact lenses[7-8].

In ophthalmic diagnostics, various methods are used to assess ocular function, including fundus photography[9], electroretinography[10], corneal topography[11], and others. Corneal topography is crucial in the fitting and monitoring of orthokeratology lenses, as it offers detailed insights into the corneal surface and the treatment's effectiveness[12]. Despite

the advancements in corneal topography technology, analyzing topography maps remains a challenging task that demands specialized knowledge and considerable time[13]. Assessing the fit of orthokeratology lenses, detecting decentration, and evaluating treatment-induced corneal changes are essential for achieving optimal vision outcomes and ensuring patient safety[14]. Manual interpretation of corneal topography in clinical practice faces several limitations: it is subjective, time-consuming, and highly dependent on clinician expertise, often resulting in variability and reduced repeatability. Complex indicators such as decentration and treatment zone size require considerable time to evaluate, which can delay diagnosis and treatment. Additionally, subtle changes in corneal curvature may be missed, particularly by less experienced clinicians who find it challenging to accurately identify complex features. These limitations highlight the need for automated, objective tools that enhance accuracy, consistency, and efficiency, streamline evaluations, and improve the management of orthokeratology treatments.

Artificial intelligence (AI) is increasingly being used in medical image analysis, leading to significant advancements in ophthalmology[15-18]. These AI algorithms have been particularly successful in various retinal imaging applications, including lesion detection[19], vascular segmentation[20], and diagnosis[21]. By streamlining processes and enhancing diagnostic accuracy, AI has the potential to greatly improve clinical outcomes and efficiency in the field.

AI-driven deep learning models in corneal topography exhibit significant potential in medical diagnostics, enabling high-accuracy analysis of extensive datasets[22-23]. For instance, Kuo *et al*[24] developed an advanced deep learning algorithm for the automatic screening of keratoconus. Shanthi *et al*[25] conducted a comprehensive review of AI applications in image segmentation and analysis, enhancing both efficiency and precision. In the domain of orthokeratology lens fitting. Fan *et al*[26] introduced a machine learning model designed to optimize orthokeratology lens fitting by interpreting corneal topography data. Koo *et al*[27] developed a machine-learning-based tool to optimize overnight orthokeratology lens fitting, while Xu *et al*[28] proposed models for both lens fitting and axial length prediction, advancing individualized treatments, advancing individualized treatments.

This study originally aims to develop and validate a multi-task AI model for automating corneal topography interpretation in orthokeratology. This research focuses on creating and validating a multi-task AI model that can accurately predict key clinical parameters from corneal topography maps. By harnessing AI's capability to detect and analyze complex patterns, the study aims to establish a robust framework for automated interpretation. This framework would facilitate the early detection of complications and optimize treatment outcomes in corneal reshaping therapy. Integrating AI in this context has the potential to significantly enhance diagnostic accuracy, streamline clinical workflows, and ultimately improve patient care by offering a more precise and efficient approach to managing orthokeratology treatments.

PARTICIPANTS AND METHODS

Ethical Approval The study was approved by the Ethics Committee of the Children's Hospital of Zhejiang University (Approval No.2024-IRB-0344-P-01) and followed the Declaration of Helsinki. Informed consent was obtained orally from the parents of all participants, and no participants received any compensation.

Dataset The study, summarized in Figure 1, involved collecting 1469 corneal topography images from 582 eyes of 326 myopic children wearing orthokeratology lenses at the Ophthalmology Department of the Children's Hospital of Zhejiang University between August 2022 and July 2024. The images were annotated by a team of 5 optometrists and 2 ophthalmologists, with discrepancies resolved through discussion to ensure consistency. The dataset was systematically divided into training (80%) and test sets (20%) using random stratified sampling to ensure balanced representation across all classification categories. The model's performance was compared to outputs from two doctors using a subset of 100 images. To further strengthen the results, external validation was carried out using 100 extra images from two different hospitals, which confirmed the model's accuracy across different datasets. Corneal topography data were collected using a Tomey corneal topographer (Tomey Corporation, Tokyo, Japan), which can capture data from up to 7936 points in less than 3s, covering a significant area of the cornea. The device features patented light-emitting cone technology and interchangeable Placido disk systems with 31 rings, allowing for high-resolution imaging and detailed topographic maps. The images were then exported as tangent images through automated scripts and corneal topography software (TMS-4A SW).

Sample Evaluation and Classification Criteria Each sample was evaluated for validity and categorized based on specific characteristics across four labels (Figure 2). Decentration: the distance between the pupil and the center of the treatment zone; a distance >0.5 mm is classified as decentration[14]. Treatment zone: The area of the corneal surface that provides functional vision, characterized by the smallest central corneal aberration and the highest visual quality. Diameters larger than 3.1 mm are labeled as "big" and those smaller than 2.8 mm are labeled as "small"[29]. Shape variation: such as bull's-eye, smiley-face (upward), sad-face (downward), and central islands.

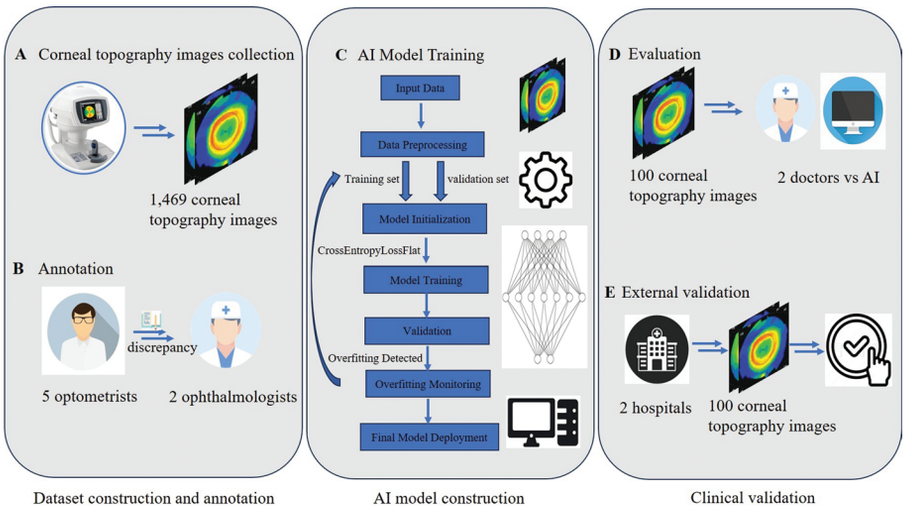

Figure 1 Flow of the study This figure outlines the workflow of the study, including data collection, annotation, model training, and validation phases. Subpanels (A, B, C, D, E) illustrate the specific stage. A: Image collection: 1469 corneal topography images were collected using the Tomey corneal topographer; B: Annotation: The images were annotated by 5 optometrists and 2 ophthalmologists, with discrepancies resolved through discussion; C: Model training: The images were split into training and validation sets. The model was trained, and overfitting was monitored; D: Evaluation: 100 images were used to compare the AI model's performance against 2 doctors; E: External validation: 100 images from two hospitals were used to validate the model's generalizability. AI: Artificial intelligence.

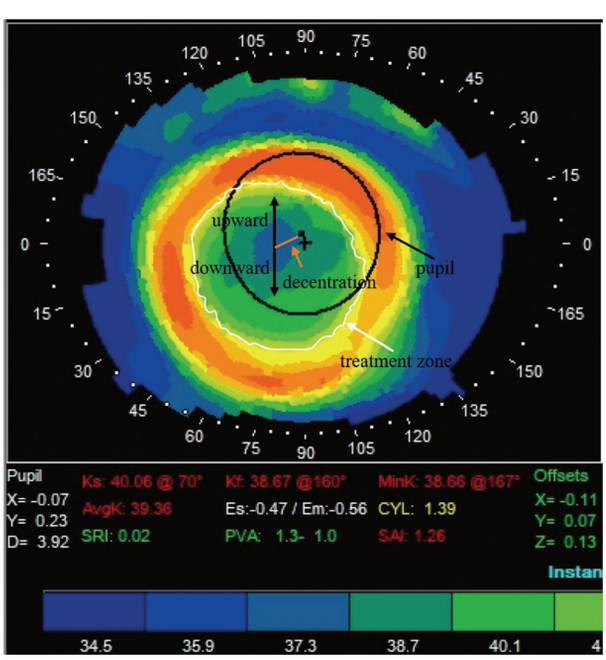

Figure 2 Tangential map after of orthokeratology lens wear This figure illustrates the treatment zone, pupil, decentration, and shape variation. Decentration: Visual representation of decentered *vs* centered treatment zones with a >0.5 mm threshold. Axes represent corneal coordinates (mm). Treatment zone size: Examples of small, moderate, and large treatment zones, with diameter thresholds (*e.g.*, <2.8 mm for small, >3.1 mm for large). Shape variation: Representative images of shape variations, including bull's-eye, smiley-face (upward), sad-face (downward), and central islands, with arrows indicating key features.

Table 1 summarizes the classification outcomes across several assessments: In the validity assessment and decentration identification, 1014 samples were deemed valid and 173 were classified as decentered, with an additional 53 decentered samples found in a subset of 229 valid samples. For treatment zone size measurement, 908 valid samples included 247 labeled as "big" and 32 as "small", while a separate cohort of 208 samples identified 62 as "big" and 12 as "small". The shape variation analysis found 22 samples with a downward shape and 12 showing other variations among 1153 valid samples, plus 5 downward shapes in a cohort of 275 samples. In the laterality of eye distribution, 606 samples came from the left eye and 581 from the right in the first group, with the second group containing 146 left-eye and 136 right-eye samples.

Table 1 Annotation of the corneal topography image dataset

Labels	Training set (80%)	Test set (20%)
Validity	1014	229
Decentration	173	53
Size	908	208
Big	247	62
Small	32	12
Shape	1153	275
Downward	22	5
Variability	12	NA
Laterality of eye		
OD	581	136
OS	606	146

NA: Not available; OD: Right eye; OS: Left eye.

Deep Learning Model Training To tackle the challenges of interpreting corneal topography, we explored a range of model architectures including ensemble models combining

ResNet18, EfficientNet_B0, and MobileNet_V2. We also investigated transformer-based models (Vision Transformers) and compared their performance with traditional convolutional neural networks (CNNs). Additionally, we implemented interpretability techniques such as Gradient-weighted class activation mapping (Grad-CAM) to visualize the model's attention on clinically relevant regions, ensuring the extraction of meaningful features aligned with clinical expertise.

The model training and validation process spanned 10 epochs, with performance metrics recorded to evaluate the effectiveness of the training regimen. Key metrics included training and validation loss, calculated using the Cross-Entropy Loss Flat function, which tracked model performance and overfitting across epochs. Furthermore, the macro F1 score was utilized to evaluate the balance between precision and recall, specifically in three essential categories: decentration detection, treatment zone evaluation, and shape variation assessment. Overall accuracy was also measured to provide a comprehensive view of the model's predictive performance. Results from each epoch, ranging from epoch 0 to 9, documented training and validation loss values, F1 scores, accuracy for each category, and the time taken per epoch. The training results indicated initially high loss values, with a noticeable decrease in training loss over subsequent epochs. Validation loss initially exhibited fluctuations, suggesting a potential overfitting scenario, which was later stabilized. The F1 scores showed progressive improvement, particularly in decentration detection and defocus evaluation, while tightness assessment exhibited minor variations. This structured approach to model training provided insights into the iterative learning process, allowing for adjustments to enhance overall performance and reliability in corneal topography predictions. Further analysis will explore the implications of these findings for clinical applications.

Comparison Between Human and AI To perform a comprehensive comparison between human expertise and the AI model's performance, 100 images were randomly selected from the test set. Two independent ophthalmologists, who were not involved in the initial labeling process, evaluated these images to ensure an unbiased assessment. Each ophthalmologist reviewed and labeled every image independently. The labels provided by both the ophthalmologists and the AI model were then compared against the original annotations, which served as the gold standard for accuracy.

External Validation To evaluate the model's generalizability and robustness across diverse clinical settings, we selected a set of 100 corneal topography images from two additional hospitals, ensuring an equal distribution of images from each institution. This dataset allowed us to test the model's performance outside the initial training environment. By including data from different hospitals, we aimed to account for variations in equipment, imaging protocols, and other contextual factors that may influence image quality and structure.

Statistical Analysis Data analysis was conducted using SPSS version 19.0 (IBM, NY, USA). The performance of the model was assessed based on accuracy, area under curve (AUC), and F1 score. AUC values were calculated for each task, and the performance of different approaches (AI only, human only, and Human+AI) was compared. Statistical significance was determined using *t*-tests for continuous variables, with a significance level set at $P<0.05$.

RESULTS

Multi-Target Loss Function Evaluation The evaluation of the multi-target loss function was conducted using a structured routing mechanism across four distinct loss configurations. Each route optimized model training by applying targeted loss weighting. Loss Routing 1 used Cross-Entropy Loss Flat with a prediction and target index of 0, applying a weight of 2.0, prioritizing accurate predictions for the primary target. Loss Routing 2 followed the same approach for the second target, maintaining balance with a weight of 2.0. Loss Routing 3 applied a weight of 1.0 to less critical predictions, with a prediction and target index of 2. Similarly, Loss Routing 4 applied a weight of 1.0 to predictions indexed at 3. These configurations aimed to enhance model performance across varied prediction tasks.

Model Performance Analysis *via* ROC Curves The receiver operating characteristic (ROC) curves display the model's classification performance across four tasks. In Task 1, the model achieves a moderate AUC of 0.64. For Task 2, performance across the "big", "small", and "moderate" classes are low, with AUC values of 0.59, 0.58, and 0.52, indicating weak discrimination. Task 3 shows mixed results, with an AUC of 0.74 for the "downward" class, while "upward" and "centered" have lower AUCs of 0.52 and 0.68, respectively. Task 4 demonstrates the strongest performance, with a high AUC of 0.95, reflecting near-perfect discrimination between the "left" and "right" classes (Figure 3).

Confusion Matrix Results The confusion matrix (CM) reveal the model's varied performance across tasks. In Task 1, the model correctly classified 60% of "decentered" samples and 55% of "centered" samples, though it showed high misclassification rates of 40%–45%. Task 2 demonstrated limited accuracy in treatment zone classification, with correct prediction rates of 40% for "big," 42% for "small", and 37% for "moderate", highlighting difficulty in differentiating size categories. Task 3 showed strong accuracy for the "downward" class at 80%, but the model failed to correctly classify any "upward" samples, and achieved only 32% accuracy for "centered". Task 4 was the model's strongest, with high accuracy rates of 88% for "left" and 90% for "right" (Figure 4).

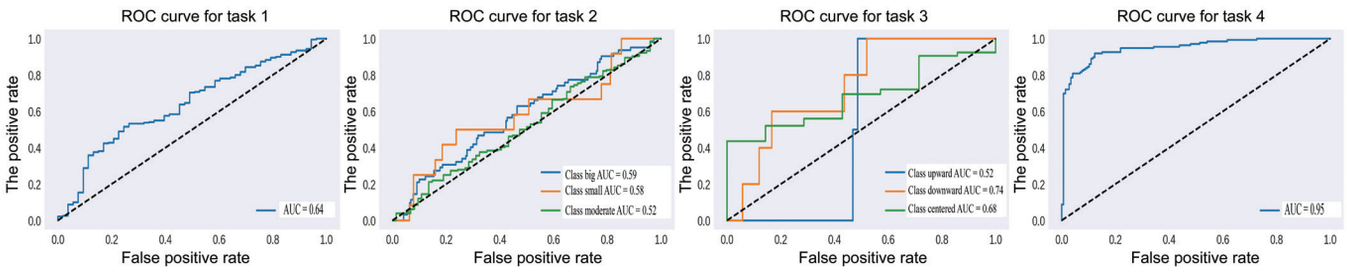

Figure 3 ROC curves for the four tasks ROC curves showing the diagnostic performance of the AI model across four distinct classification tasks. Each curve plots the true positive rate against the false positive rate at different threshold settings. ROC: Receiver operating characteristic; AUC: Area under the curve; AI: Artificial intelligence.

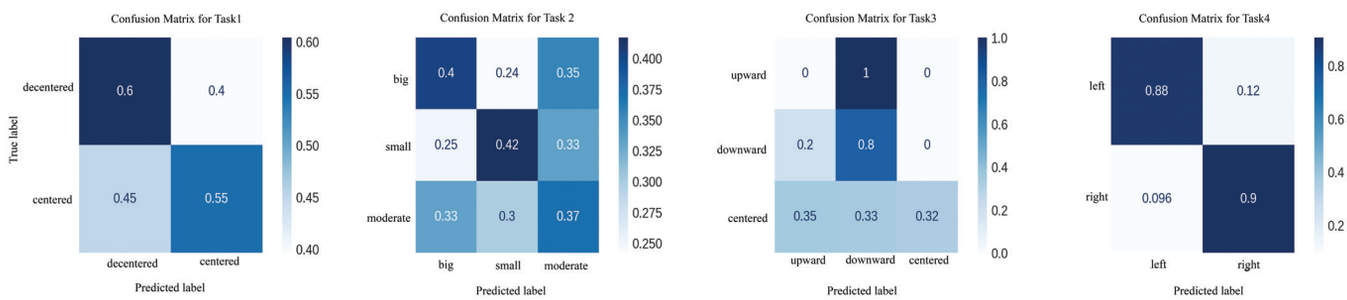

Figure 4 CM results for the four tasks The CM shows performance across four tasks. Rows represent true labels, columns represent predicted labels, and values are percentages of total samples for each true class. CM: Confusion matrix.

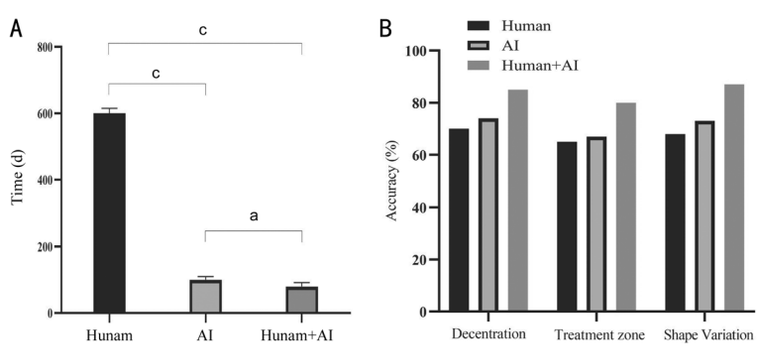

Figure 5 Comparison of human and AI performance in interpreting corneal topography maps Evaluation of test set performance on 100 corneal topography maps, including time taken (A) and accuracy metrics (B) for decentration, treatment zone, and shape variation. Bar charts compare the accuracy and processing speed of AI, human, and combined approaches across classification tasks. [a]*P*<0.05, [c]*P*<0.001. AI: Artificial intelligence.

Comparison Between Human and AI Performance The comparison between human, AI, and Human+AI approaches shows that the combined Human+AI method delivers the highest accuracy across all tasks—85% for decentration, 73% for treatment zone, and 87% for shape variation—outperforming both human-only and AI-only methods. Additionally, Human+AI achieves the fastest processing time at 80ms, even faster than AI alone (100ms) and significantly faster than humans alone (600ms). This suggests that integrating human expertise with AI capabilities optimizes both speed and accuracy, making the Human+AI approach the most effective overall (Figure 5).

External Validation Results The external validation results reveal varying levels of model performance across four tasks. The model performs best in Task 4, achieving high accuracy (over 90%) with minimal misclassification between left and right eyes. Task 1 shows moderate accuracy but faces notable misclassification issues, with some overlap between "decentered" and "centered" categories. Task 2 has inconsistent accuracy across "big", "small", and "moderate" classes, highlighting challenges in distinguishing treatment zone sizes. Task 3 performs well in the "upward" class but struggles with "downward" and "centered" categories. Overall, while the model is robust in laterality of eye prediction, it requires further refinement to improve accuracy in more nuanced categories across other tasks (Figure 6).

DISCUSSION

The model's AUC values (0.52–0.74) suggest suboptimal performance in complex tasks, although it showed high accuracy in distinguishing eye laterality (AUC of 0.95). Its challenges in tasks like decentration, treatment zone size, and shape variation stem from the difficulty of classifying subtle

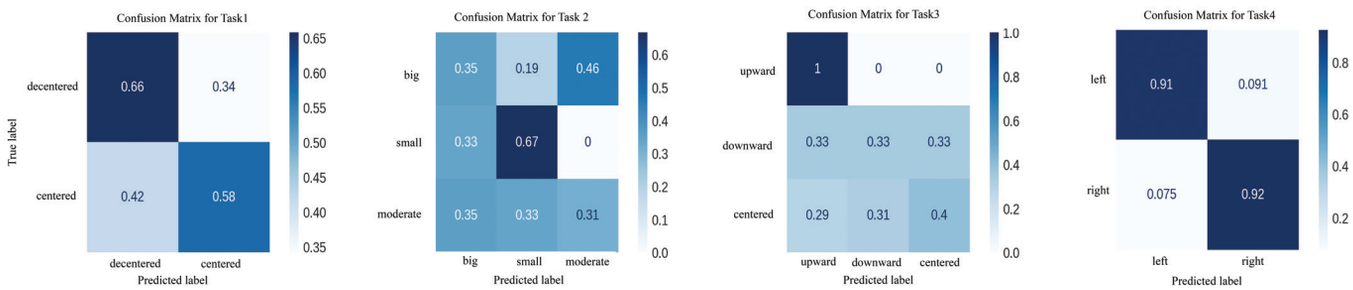

Figure 6 CM for four tasks during external validation The CM shows performance across four tasks during external validation using data from two hospitals. Rows represent true labels, columns represent predicted labels, and values are percentages of total samples. CM: Confusion matrix.

variations in corneal topography, indicating a need for further refinement. Despite these limitations, the approach shows promise in improving corneal topography interpretation, particularly for orthokeratology, by enhancing precision and efficiency in pediatric myopia management. However, it should be seen as an assistive tool rather than a standalone diagnostic solution at this stage.

The model demonstrated an excellent ability to distinguish between left and right eye data in Task 4, achieving an AUC of 0.95 with very few misclassifications. The result highlights the potential for AI to automate simpler tasks, like predicting the side of the eye, with high accuracy. The success of this task can be linked to the distinct and recognizable features of eye anatomy, particularly those visible in corneal topography[30-31]. These results are consistent with earlier research, which has also emphasized the strength of AI in analyzing anatomical features in ophthalmic imaging[32].

However, the model's performance in predicting decentration (Task 1), treatment zone size (Task 2), and shape variation (Task 3) showed inconsistencies. AUC scores for these tasks varied significantly, ranging from 0.52 to 0.74. This spread suggests a high degree of misclassification, particularly in the task of predicting treatment zone size, where categories were often incorrectly identified. The confusion matrices highlighted notable overlaps between categories, especially for "small", "big", and "moderate" reflecting the difficulty the model faced in distinguishing between these specific groups. These findings suggest that the model may be experiencing overfitting to specific patterns or failing to learn meaningful clinical features, indicating the need for improved training strategies and potentially more diverse datasets.

The findings indicate that distinguishing these classes using current AI models is challenging, reflecting earlier research on the difficulties of classifying complex anatomical variations. This issue is well-documented in the broader field of AI applications in medical imaging. Segmentation and classification tasks are often hampered by the intricate and variable nature of anatomical structures. For example, a review on AI in medical imaging highlights that while CNNs show significant promise in these areas, they still face challenges with generalizability and accuracy, especially in complex cases with subtle anatomical differences[33]. Another study reviewing AI techniques in disease classification and segmentation also notes the difficulties in model generalization across different anatomical regions. This underscores the need for hybrid approaches that combine machine learning and deep learning techniques to improve performance in diverse medical imaging tasks[34].

The challenges faced by AI models in predicting decentration, treatment zone size and subtle shape variations may stem from factors such as data imbalance, annotation subjectivity, and subtle feature variations. To address these challenges, strategies such as expanding and diversifying the dataset, refining ensemble learning, and applying task-specific data augmentation can be implemented. Some recent research has explored ensemble learning systems for keratoconus diagnosis, pointing out that combining multi-task learning with additional training data can improve accuracy by using a wider range of data, making the models more robust[35]. Additionally, there has been progress in developing deep learning models for predicting corneal topography changes during orthokeratology, where spatially distributed data has proven to offer better predictive power, emphasizing the need for increasingly advanced algorithms[36]. Even though these complex cases pose challenges, AI has demonstrated its usefulness in handling simpler tasks, providing valuable support to clinical evaluations. Some studies propose integrating AI models into clinical practices, especially in fields like orthokeratology and keratoconus detection, as long as these models are enhanced through methods like ensemble learning and the use of more diverse datasets[37]. This suggests that with further refinement, AI could become a critical tool in more intricate analyses.

The comparison between human experts and the AI model highlights the strengths of each approach. AI excelled in efficiency and accuracy for routine tasks, while the combined Human+AI approach achieved the highest overall accuracy

across all tasks—85% for decentration, 73% for treatment zone, and 87% for shape variation—and was the fastest, processing at 80ms, compared to 100ms for AI alone and 600 ms for human-only assessments. External validation using data from two additional hospitals confirmed high AI accuracy (over 90%) for straightforward tasks like laterality of eye prediction. However, performance dropped in more nuanced tasks, likely due to differences in imaging protocols, underscoring the need for further refinement to improve AI's adaptability across varied clinical environments.

Despite its potential, ethical concerns about AI in diagnostics remain[38]. These include the risk of over-relying on flawed models, which can lead to inaccurate diagnoses, especially with biased or incomplete data. The "black box" nature of AI reduces transparency and accountability[39], making it difficult for clinicians to understand how decisions are made. Additionally, there is concern that AI might diminish human expertise, particularly in complex cases. Therefore, ensuring patient data privacy, using diverse datasets, and addressing bias are crucial to prevent disparities and maintain ethical standards in AI-assisted diagnostics.

This study has several limitations. First, the dataset is primarily derived from a single institution and has a limited sample size, which may restrict the generalizability of the AI model to other clinical settings with varying imaging protocols. Additionally, the AI encountered challenges in more nuanced classifications, such as treatment zone size and subtle shape variations, underscoring its sensitivity to overlapping feature spaces. Finally, while external validation was performed, further multi-center studies with larger and more diverse datasets are needed to enhance the model's robustness and adaptability across varied clinical environments.

In summary, while AI shows promise for routine tasks in corneal topography, the current model requires significant optimization before clinical implementation. More complex classifications, such as subtle decentrations and treatment zone variations, benefit from a Human+AI collaborative approach. However, the system is currently unable to reliably replace human expertise in complex classifications. Unless significant improvements in accuracy are achieved, its role remains assistive rather than diagnostic. Future improvements, such as incorporating data from multiple hospitals, increasing the sample size, ensemble learning, model tuning, and feature engineering, could further enhance AI's robustness. This would solidify the Human+AI model as a valuable tool in orthokeratology, improving diagnostic accuracy and efficiency in patient care.

ACKNOWLEDGEMENTS

Foundation: Supported by the National Natural Science Foundation of China (No.82201195).

Conflicts of Interest: Kang DH, None; **Yuan L,** None; **Feng J,** None; **Zhan J,** None; **Grzybowski A,** None; **Sun W,** None; **Jin K,** None.

REFERENCES

1 Baird PN, Saw SM, Lanca C, *et al*. Myopia. *Nat Rev Dis Primers* 2020;6:99.

2 Wong YL, Saw SM. Epidemiology of pathologic myopia in Asia and worldwide. *Asia Pac J Ophthalmol* (*Phila*) 2016;5(6):394-402.

3 Dong L, Kang YK, Li Y, *et al*. Prevalence and time trends of myopia in children and adolescents in China: a systemic review and Meta-analysis. *Retina* 2020;40(3):399-411.

4 Naidoo KS, Fricke TR, Frick KD, *et al*. Potential lost productivity resulting from the global burden of myopia: systematic review, meta-analysis, and modeling. *Ophthalmology* 2019;126(3):338-346.

5 Wang SK, Guo YF, Liao CM, *et al*. Incidence of and factors associated with myopia and high myopia in Chinese children, based on refraction without cycloplegia. *JAMA Ophthalmol* 2018;136(9):1017-1024.

6 Feifei S, Huifeng W, Feidi L, *et al*. Study on the myopia control effect of OK lens on children with different corneal curvature. Published online April 16, 2024. https://www.researchsquare.com/article/rs-4247883/v1

7 Charm Chi Foon J. Orthokeratology: clinical utility and patient perspectives. *Clin Optom* 2017;9:33-40.

8 Zhang J, Li J, Li XF, *et al*. Redistribution of the corneal epithelium after overnight wear of orthokeratology contact lenses for myopia reduction. *Cont Lens Anterior Eye* 2020;43(3):232-237.

9 Su S, Wu J, Ji M, *et al*. Comparison of three fundus inspection methods during phacoemulsification in diabetic white cataract. *Int J Ophthalmol* 2023;16(11):1782-1788.

10 Kremers J, Huchzermeyer C. Electroretinographic responses to periodic stimuli in Primates and the relevance for visual perception and for clinical studies. *Vis Neurosci* 2024;41:E004.

11 Galindo-Ferreiro A, De Miguel-Gutierrez J, González-Sagrado M, *et al*. Validity of autorefractor based screening method for irregular astigmatism compared to the corneal topography- a cross sectional study. *Int J Ophthalmol* 2017;10(9):1412-1418.

12 Nti AN, Berntsen DA. Optical changes and visual performance with orthokeratology. *Clin Exp Optom* 2020;103(1):44-54.

13 Klyce SD. Developments in corneal topographic analysis following contact lens wear and refractive surgery. *Cont Lens Anterior Eye* 2001;24(4):168-174.

14 Zhang SX, Zhang H, Li LH, *et al*. Effect of treatment zone decentration on axial length growth after orthokeratology. *Front Neurosci* 2022;16:986364.

15 Gao ZY, Pan XJ, Shao J, *et al*. Automatic interpretation and clinical evaluation for fundus fluorescein angiography images of diabetic retinopathy patients by deep learning. *Br J Ophthalmol* 2023;107(12):1852-1858.

16 Jin K, Grzybowski A. Advancements in artificial intelligence for the diagnosis and management of anterior segment diseases. *Curr Opin Ophthalmol* 2025;36(4):335-342.

17 Biswas A, Banik R. Advancements in medical image analysis: a comprehensive method of AI-based classification and segmentation technique. *Artif Intell Appl* 2024.

18 Jin K, Ye J. Artificial intelligence and deep learning in ophthalmology: Current status and future perspectives. *Adv Ophthalmol Pract Res* 2022;2(3):100078.

19 Kijowski R, Liu F, Caliva F, *et al*. Deep learning for lesion detection, progression, and prediction of musculoskeletal disease. *J Magn Reson Imaging* 2020;52(6):1607-1619.

20 Shin SY, Lee S, Yun ID, *et al*. Deep vessel segmentation by learning graphical connectivity. *Med Image Anal* 2019;58:101556.

21 Li JO, Liu HR, Ting DSJ, *et al*. Digital technology, tele-medicine and artificial intelligence in ophthalmology: a global perspective. *Prog Retin Eye Res* 2021;82:100900.

22 Keshavarz M, Ahmadi MJ, Naseri SS, *et al*. AI-driven keratoconus detection: integrating medical insights for enhanced diagnosis. *2023 11th RSI International Conference on Robotics and Mechatronics (ICRoM)*. December 19-21, 2023, Tehran, Iran, Islamic Republic of. IEEE, 2023:654-660.

23 Fassbind B, Langenbucher A, Streich A. Automated cornea diagnosis using deep convolutional neural networks based on cornea topography maps. *Sci Rep* 2023;13(1):6566.

24 Kuo BI, Chang WY, Liao TS, *et al*. Keratoconus screening based on deep learning approach of corneal topography. *Transl Vis Sci Technol* 2020;9(2):53.

25 Shanthi S, Aruljyothi L, Balasundaram MB, *et al*. Artificial intelligence applications in different imaging modalities for corneal topography. *Surv Ophthalmol* 2022;67(3):801-816.

26 Fan YZ, Yu ZK, Tang T, *et al*. Machine learning algorithm improves accuracy of ortho-K lens fitting in vision shaping treatment. *Cont Lens Anterior Eye* 2022;45(3):101474.

27 Koo S, Kim WK, Park YK, *et al*. Development of a machine-learning-based tool for overnight orthokeratology lens fitting. *Transl Vis Sci Technol* 2024;13(2):17.

28 Xu S, Yang XY, Zhang SX, *et al*. Machine learning models for orthokeratology lens fitting and axial length prediction. *Ophthalmic Physiol Opt* 2023;43(6):1462-1468.

29 Carracedo G, Espinosa-Vidal TM, Martínez-Alberquilla I, *et al*. The topographical effect of optical zone diameter in orthokeratology contact lenses in high myopes. *J Ophthalmol* 2019;2019:1082472.

30 Anton N, Doroftei B, Curteanu S, *et al*. Comprehensive review on the use of artificial intelligence in ophthalmology and future research directions. *Diagnostics* (*Basel*) 2022;13(1):100.

31 Xu S, Yang XY, Zhang SX, *et al*. Evaluation of the corneal topography based on deep learning. *Front Med* 2023;10:1264659.

32 Lopes BT, Eliasy A, Ambrosio R. Artificial intelligence in corneal diagnosis: where are we? *Curr Ophthalmol Rep* 2019;7(3):204-211.

33 Breesam AM, Adnan SR, Ali SM. Segmentation and classification of medical images using artificial intelligence: a review. *Al Furat J Innov Electron Comput Eng* 2024;3(2):299-320.

34 Azizi A, Azizi M, Nasri M. Artificial intelligence techniques in medical imaging: a systematic review. *Int J Onl Eng* 2023;19(17):66-97.

35 Ghaderi M, Sharifi A, Jafarzadeh Pour E. Proposing an ensemble learning model based on neural network and fuzzy system for keratoconus diagnosis based on Pentacam measurements. *Int Ophthalmol* 2021;41(12):3935-3948.

36 Rong DY, Zhao ZY, Wu Y, *et al*. Prediction of myopia eye axial elongation with orthokeratology treatment *via* dense I2I based corneal topography change analysis. *IEEE Trans Med Imaging* 2024;43(3):1149-1164.

37 Al-Timemy AH, Ghaeb NH, Mosa ZM, *et al*. Deep transfer learning for improved detection of keratoconus using corneal topographic maps. *Cogn Comput* 2022;14(5):1627-1642.

38 Evans NG, Wenner DM, Cohen IG, *et al*. Emerging ethical considerations for the use of artificial intelligence in ophthalmology. *Ophthalmol Sci* 2022;2(2):100141.

39 Ting DSW, Al-Aswad LA. Augmented intelligence in ophthalmology: the six rights. *Asia Pac J Ophthalmol* (*Phila*) 2021;10(3):231-233.